A Microwave-Powered Thermospray Nebulizer for Liquid Sample Introduction in Inductively Coupled Plasma Atomic Emission Spectrometry

ARTICLE *in* ANALYTICAL CHEMISTRY · SEPTEMBER 1997

Impact Factor: 5.64 · DOI: 10.1021/ac961247a · Source: PubMed

5 AUTHORS, INCLUDING:

José Luís Todolí
University of Alicante
83 PUBLICATIONS **1,105** CITATIONS
SEE PROFILE

Juan Mora
University of Alicante
50 PUBLICATIONS **815** CITATIONS
SEE PROFILE

Antonio Canals
University of Alicante
116 PUBLICATIONS **2,495** CITATIONS
SEE PROFILE

Vicente Hernandis
University of Alicante
40 PUBLICATIONS **901** CITATIONS
SEE PROFILE

Anal. Chem. **1997,** *69,* 3578−3586

A Microwave-Powered Thermospray Nebulizer for Liquid Sample Introduction in Inductively Coupled Plasma Atomic Emission Spectrometry

Luis Bordera, José L. Todolí, Juan Mora, Antonio Canals,* and Vicente Hernandis

Departamento de Química Analítica, Universidad de Alicante, E-03071 Alicante, Spain

A new thermospray nebulizer based on the absorption of microwave radiation (MWTN) by aqueous solutions of strong acids is presented for the first time. To this end, a given length of the sample capillary is placed inside the cavity of a focused microwave system. A small piece of a narrower capillary tubing is connected at the tip of the sample capillary, outside the microwave cavity, to build up pressure. Drop size distributions of primary aerosols are exhaustively measured in order to evaluate the influence of several experimental variables (microwave power, liquid flow, irradiation length, inner diameter of the outlet capillary, nature and concentration of the acid) on the characteristics of the primary aerosol that are related to the emission signal. These experiments have been performed mainly to increase our understanding of the microscopic process of this new type of aerosol generation. A standard Meinhard nebulizer was employed for comparison. Under the best conditions the entire aerosol volume is contained in droplets smaller than 20 μm compared with 45% of the volume of the aerosol generated by the Meinhard. Hence, higher analyte and aerosol transport rates are to be expected for the MWTN compared with the Meinhard nebulizer. As any highly efficient nebulizer, MWTN requires a desolvation unit. For solutions 0.75 M in strong acid, the new nebulizer improves sensitivity (1.0−2.8 times), limits of detection (1.2−3.0 times), and background equivalent concentration (0.9−2.0 times) as compared to the standard Meinhard nebulizer, features many of the advantages of the conventional thermospray nebulizer, and overcomes some of its drawbacks (MWTN does not show corrosion problems and works at lower pressure, the aerosol characteristics are not modified when the PTFE capillary is replaced).

The introduction of samples as aerosols has many advantages in inductively coupled plasma atomic emission spectrometry (ICPAES).[1,2] The conversion of a liquid bulk into an aerosol is usually done by means of a pneumatic nebulizer. In some cases, the performance of the pneumatic nebulization is not as good as required. In such situations, one should turn to more efficient nebulizers (i.e., ultrasonic nebulizer, hydraulic high-pressure nebulizer, single-bore high-pressure nebulizer, pneumatic high-efficiency nebulizer, thermospray nebulizer, etc.). Among them, the thermospray nebulizer (TN)[3] is a good choice because it generates a hot and very fine primary aerosol,[4] thus causing a high percentage of the analyte to reach the atomization cell.[5] It shows much better analytical behavior than conventional pneumatic nebulizers in terms of sensitivity and limits of detection (LOD).[6−8] Nevertheless, the TN is not well suited to working with acidic or high salt content solutions and slurries.[7,9] One remedy that has been proposed to avoid contamination problems due to capillary corrosion is to place a silica capillary inside the stainless steel capillary.[10−12] This additional operation, however, reduces heat transmission.

Microwave (MW) radiation has proved to be an attractive alternative to the conventional heating methods for sample treatment or digestion.[13−15] Microwave heating is based on dipole rotation and ion migration.[16] Hence, for a solution, heating efficiency is expected to increase with solvent polarity and with ionic conductance and concentration. An excellent review devoted to new analytical applications of microwave radiation has been recently published.[17]

One of the potential applications of MW radiation is its use for aerosol generation, in the form of a microwave-powered thermospray nebulizer (MWTN),[18,19] which is the aim of this paper. To our knowledge, this is the first time that the absorption of MW radiation by the sample solution has been applied to aerosol generation in atomic spectrometry.

(1) Sneddon, J., Ed. *Sample introduction in atomic spectroscopy*; Elsevier: New York, 1990.
(2) Browner, R. F. *Microchem. J.* **1989**, *40*, 4−29.
(3) Vestal, M. L.; Fergusson, G. J. *Anal. Chem.* **1985**, *57*, 2373−2378.
(4) Schwartz, S. A.; Meyer, G. A. *Spectrochim. Acta* **1986**, *41B*, 1287−1298.
(5) Koropchak, J. A.; Winn, D. H. *Appl. Spectrosc.* **1987**, *41*, 1311−1318.
(6) Meyer, G. A.; Roeck, J. S.; Vestal, M. L. *ICP Inf. Newsl.* **1985**, *10*, 955−963.
(7) Koropchak, J. A.; Veber, M. *Crit. Rev. Anal. Chem.* **1992**, *23*, 113−141.
(8) Thomas, C.; Jakubowski, N.; Stüwer, D.; Broekaert, J. A. C. *J. Anal. At. Spectrom.* **1995**, *10*, 583−590.
(9) Elgersma, J. W.; Maessen, F. J. M. J.; Niessen, M. A. *Spectrochim. Acta* **1986**, *41B*, 1217−1220.
(10) Veber, M.; Koropchak, J. A.; Conver, T.; Herries, J. *Appl. Spectrosc.* **1992**, *46*, 1525−1531.
(11) de Loos-Vollebregt, M. T. C.; Peng, R.; Tiggelman, J. J. *J. Anal. At. Spectrom.* **1991**, *6*, 165−168.
(12) Peng, R.; Tiggelman, J. J.; de Loos-Vollebregt, M. T. C. *Spectrochim. Acta* **1990**, *45B*, 189−199.
(13) Abu-Samra, A; Morris, J. S.; Koirtyohann, S. R. *Anal. Chem.* **1975**, *47*, 1475−1477.
(14) Copson, D. A. *Microwave Heating*, 2nd ed.; AVI: Westport, CT, 1975.
(15) Bordera, L.; Hernandis, V.; Canals, A. *Fresenius' J. Anal. Chem.* **1996**, *355*, 112−119.
(16) Kingston, H. M., Jassie, L. B., Eds. *Introduction to Microwave Sample Preparation. Theory and Practice*; American Chemical Society: Washington, 1988.
(17) Zlotorzynski, A. *Crit. Rev. Anal. Chem.* **1995**, *15*, 43−76.
(18) Hernandis, V.; Canals, A.; Todolí, J. L.; Bordera, L. Patent No. P95-00809, Spain, 1995.
(19) Bordera, L.; Todolí, J. L.; Mora, J.; Canals, A.; Hernandis, V. *J. Aerosol Sci.* **1996**, *27*, S387−S388.

S0003-2700(96)01247-4 CCC: $14.00

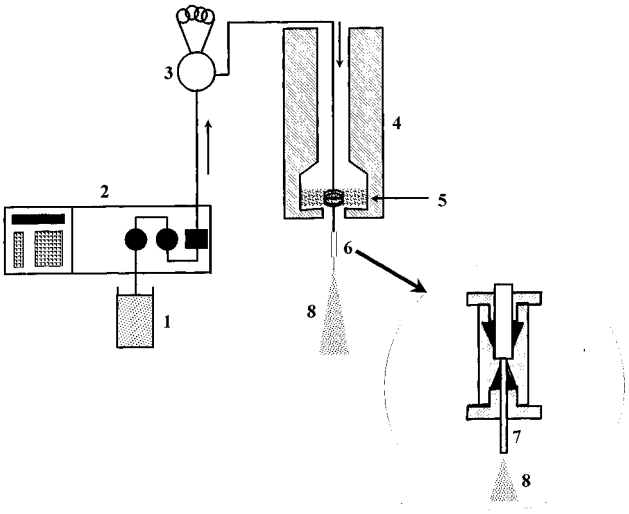

Figure 1. Schematic diagram of the experimental assembly for the microwave powered thermospray (MWTN): (1) carrier stream (water); (2) HPLC pump; (3) PTFE valve and loop; (4) focused microwave oven; (5) irradiated volume; (6) PEEK union; (7) outlet capillary; (8) aerosol.

The goal of this study was to evaluate this new microwave thermospray nebulizer for the introduction of acidic solutions in ICPAES. To this end, the influence of several variables (MW power, liquid flow, irradiation length, inner diameter of the outlet capillary, and acid nature and concentration) on the characteristics of the primary aerosols and on the analytical behavior in ICPAES was studied.

EXPERIMENTAL SECTION

Nebulizer Description and Operating Principle. Figure 1 shows a schematic diagram of the experimental assembly of the MWTN. In this first design, the main component is a focused microwave oven (4) inside of which a given length of PTFE capillary (0.5 mm i.d., 1.6 mm o.d.) has been placed. PTFE was chosen because it is almost transparent to MW radiation, withstands temperatures well above the boiling points of the solvents employed, and is very inert. This capillary emerges through the bottom of the oven. There, a small piece of a narrower capillary tubing, made of PTFE or fused silica (7), is connected to the end of the first one by means of a PEEK union (6). Hereinafter, this small capillary will be called the outlet capillary.

The operating principle of the MWTN is as follows: The carrier solution (1) is forced to pass along the conduction by means of an HPLC pump (2). At the appropriate time, the acidic sample solution is injected into the carrier stream by means of a valve (3). The carrier with the sample is introduced in a focused microwave oven (4). Once the solution reaches the irradiated volume (5), it begins to heat and to boil at a rate that depends on its composition, thus causing the pressure inside the capillary to increase since the outlet capillary (7) imposes a restriction. The solution is partially evaporated in the irradiation step. Thus, the remaining liquid sample is exposed to a stream of evaporated solvent flowing at high velocity. Finally, the gas and liquid mixture emerges from the outlet capillary and expands, thus giving rise to a fine, hot aerosol (8).

MW heating does not require previous heating of the capillary walls. The capillary is made of PTFE, which does not absorb microwave radiation. In fact, MW absorption takes place in the whole liquid vein. Therefore, in a cross section of the liquid vein, all the points are heated at about the same rate and their temperatures are expected to be similar, since the penetration depth of the microwave radiation (14 mm at 25 °C and 57 mm at 95 °C) is very much higher than the inner radius of the capillary (0.25 mm). By contrast, in a conventional thermospray, heating is carried out by conduction and convection, so that the temperature of the liquid vein decreases from the walls to the central axis.

Due to its characteristics, the MWTN is perfectly well suited to handle highly acidic solutions for long periods of time. It is even reasonable to expect that an increase in the ionic concentration of the solution would accelerate the heating process without disturbing the nebulization.

Table 1. Viscosities, Ionic Strengths, and Densities of the Solutions Employed

acid	concn (M)	rel viscosity[a]	ionic strength	density[a] (g/mL)
nitric	0.75	1.01	0.75	1.024
nitric	1.50	1.04	1.50	1.049
nitric	3.00	1.11	3.00	1.100
nitric	6.00	1.35	6.00	1.192
hydrochloric	0.75	1.04	0.75	1.012
hydrochloric	1.50	1.08	1.50	1.026
hydrochloric	3.00	1.17	3.00	1.050
hydrochloric	6.00	1.37	6.00	1.098
perchloric	0.75	0.92	0.75	1.036
perchloric	1.50	0.91	1.50	1.076
perchloric	3.00	0.97	3.00	1.162
perchloric	6.00	1.03	6.00	1.309
sulfuric	0.75	1.16	0.96	1.046
sulfuric	1.50	1.32	1.74	1.091
sulfuric	3.00	1.75	3.34	1.179
sulfuric	6.00	3.06	6.40	1.338
phosphoric	0.75	1.03	0.07	1.006
phosphoric	1.50	1.47	0.10	1.075
phosphoric	3.00	2.16	0.14	1.150
phosphoric	6.00	3.89	0.20	1.454

[a] Relative viscosities were obtained as η/η_o, where η_o is the water viscosity at 20 °C. Relative viscosities and densities of $HClO_4$ were obtained experimentally, while the rest were taken from *CRC Handbook of Chemistry and Physics*, 70th ed.; Weast, R. C., Ed.; CRC Press, Inc.: Boca Raton, FL, 1989.

Reagents and Instrumentation. Five acids, HNO_3, H_2SO_4, HCl, $HClO_4$, and H_3PO_4, were employed in concentrations ranging from 0.75 to 6.0 M. These solutions were prepared from their respective concentrated commercial solutions (Merck, Darmstadt, Germany). Table 1 lists the relative viscosities, ionic strengths, and densities of the solutions employed.

Pure water was continuously fed by means of an HPLC pump (Spectra Physics, Model IsoChrom LC, San Jose, CA). The sample solution was inserted in the water stream by means of a PTFE-lined valve (Omnifit, Model 1106, Cambridge, UK) equipped with a PTFE loop, the volume of which was 12 mL. In this first design, a focused MW oven (Prolabo, Model Maxidigest MX350, Paris, France) was employed as the heating system, operating at a frequency of 2450 MHz. Two outlet capillaries, one made of PTFE (100 μm i.d.) and the other made of fused silica (75 μm i.d.) were employed. A mass flow controller (Tylan, Model FC-260, Torrance, CA) was used to control the argon carrier/nebulizer gas flow.

The results obtained with the MWTN were compared with those obtained with a Meinhard nebulizer (Meinhard Associates

Inc., Model TR-30-A3, CA), for which the cross section of the gas outlet was 2.83×10^{-2} mm^2.

The characteristics of the MWTN do not allow a direct coupling of this nebulizer to the introduction system of the ICP instrument (i.e., a conventional double-pass Scott chamber and the injector tube of the torch). Because of this, the aerosol generated by the MWTN was driven to the plasma through a nonthermostated single-pass chamber, and a condensation unit formed by two Liebig condensers (both 20 cm long and 1.5 cm i.d.), the first one kept at 20 °C with tap water and the second at 1 °C by means of a thermostatic bath (Haake, Model F3-K, Karlsruhe, Germany). This system greatly reduces the solvent load to the plasma, since the MWTN generates large amounts of solvent vapor. Otherwise, the excitation characteristics of the plasma would be seriously hampered. The Meinhard nebulizer has been used in the usual configuration of the introduction system, i.e., in conjunction with a double-pass Scott chamber ($V = 120$ cm^3) placed at the torch base, without a desolvation unit.

The drop size distributions of the primary aerosols (pDSD) were measured by means of a laser Fraunhofer diffraction system (Malvern Instruments Ltd., Model 2600c, Worcestershire, UK) equipped with a lens, the focal length of which was 63 mm, that allowed for the measurement of drop diameters ranging from 1.2 to 118 μm. Software version B.0D was employed for the calculations. The transformation from energy distribution to drop size distribution was done using a model-independent algorithm (i.e., an algorithm that is not based on any distribution model). Primary aerosols were measured at a distance of 10 mm from the tip of the nebulizers. For a better understanding of the effect of the variables, in some cases, the whole primary drop size distribution curves have been shown. These primary drop size distributions have been displayed on an absolute volume basis.[20] To do this, the drop size distribution curves show the volume of aerosol contained in a given drop size interval ($\Delta B/\Delta \log d$) as a function of the drop size (d). The ΔB values were calculated by multiplying the so-called volume concentration (VC) of the aerosol by the percentage of the aerosol volume contained in a given drop size interval. The volume concentration gives the percentage of the active volume of the laser beam that is actually occupied by liquid droplets.[21] Hence, it provides a measurement of the amount of solvent in liquid form in the active volume. Therefore, the area under the drop size distribution curves is proportional to the total volume of aerosol present in the active volume of the laser beam. However, these curves do not include the volume of aerosol contained in droplets smaller than 1.2 μm, since they are out of the scope of the instrument.

The median of the volume distribution (D_{50}) was used to measure the central tendency or position of the pDSD on the X-axis. The dispersion of the drop size distribution curves was accounted for by means of their "width" ($D_{90}-D_{10}$) and their span values.[21,22] The common spray chambers, such as the double-pass Scott type, are very efficient in removing large droplets (for instance, larger than 20 μm) from the primary aerosol.[23] Hence, the volume percentage of the aerosol contained in droplets smaller than 20 μm (V_{20}) has been chosen in order to try to correlate the characteristics of the primary aerosols to the transport rate. This way, the greater the value of V_{20} is, the greater the volume of liquid aerosol that can be transported to the plasma will be.

The back-pressure (P_1) due to the MW nebulization was also measured in order to evaluate the amount of energy inside the MWTN. To this end, the HPLC pressure readings when the MW oven was off (no nebulization) and when it was on (nebulization) were recorded.

Atomic emission intensity was measured using an ICP spectrometer (Baird, Model 2070, Bedford, MA). Table 2 lists the instrumental conditions. For the MWTN, the sample solution contained 1.0 μg/mL of each of 10 elements and was 0.75 M in HNO_3, $HClO_4$, HCl, or H_2SO_4, while for the Meinhard, only HNO_3 (0.75 M) was used. Table 3 lists the wavelength and slit width chosen for each element.

Table 2. Instrumental Conditions[a]

ICPAES Instrument	
forward power (kW)	1.2
outer argon flow rate (L/min)	15
intermediate argon flow rate (L/min)	1.6
carrier/nebulizer gas flow rate (L/min)	0.54
observation height (mm above load coil)	8
integration time (s)	0.2
Aerosol Transport System	
spray chamber[b]	single-pass (vol, 40 cm^3)
condensation temp of system (°C)	
first step	20
second step	1

[a] Optimized for both sample introduction systems (see text for explanation). [b] With the Meinhard nebulizer, a double-pass spray chamber (120 cm^3) was also used.

Table 3. Wavelengths and Slit Widths for the Elements Studied

element	wavelength (nm)	slit width[a] (nm)
Al I	309.271	0.4
Ba II	455.403	0.3
Ca II	393.366	0.2
Cd I	228.802	0.5
Cr II	283.563	0.4
Cu I	324.754	0.3
Fe II	259.940	0.3
Mg II	279.553	0.4
Mn II	257.610	0.3
Zn I	213.856	0.4

[a] Optimized for each line.

RESULTS AND DISCUSSION

Drop Size Distributions of the Primary Aerosols. (1) Influence of MW Power. Figure 2A shows the pDSD for a HNO_3 solution operating at two different MW powers, whereas (B) and (C) show the variation of D_{50} and P_1, respectively, vs the applied MW power for solutions 0.75 M in HNO_3, $HClO_4$, HCl, and H_2SO_4. Phosphoric acid has not been included here since, under the experimental conditions corresponding to these figures, no aerosol was generated.

Figure 2A shows that the pDSD corresponding to the highest power value (300 W) is slightly shifted to smaller droplet diameters. Drop size distributions peak at 12.0 and 16.2 μm, respectively, for powers of 300 and 150 W. As regards the

(20) Mora, J.; Canals, A.; Hernandis, V. *Spectrochim. Acta* **1996**, *51B*, 1535−1549.
(21) Malvern Instruments Particle Sizer Reference Manual, Version B.0D.
(22) Lefebvre, A. H. *Atomization and Sprays*; Hemisphere: New York, 1989.
(23) Olesik, J. W.; Kinzer, J. A.; Harkleroad, B. *Anal. Chem.* **1994**, *66*, 2022−2030.

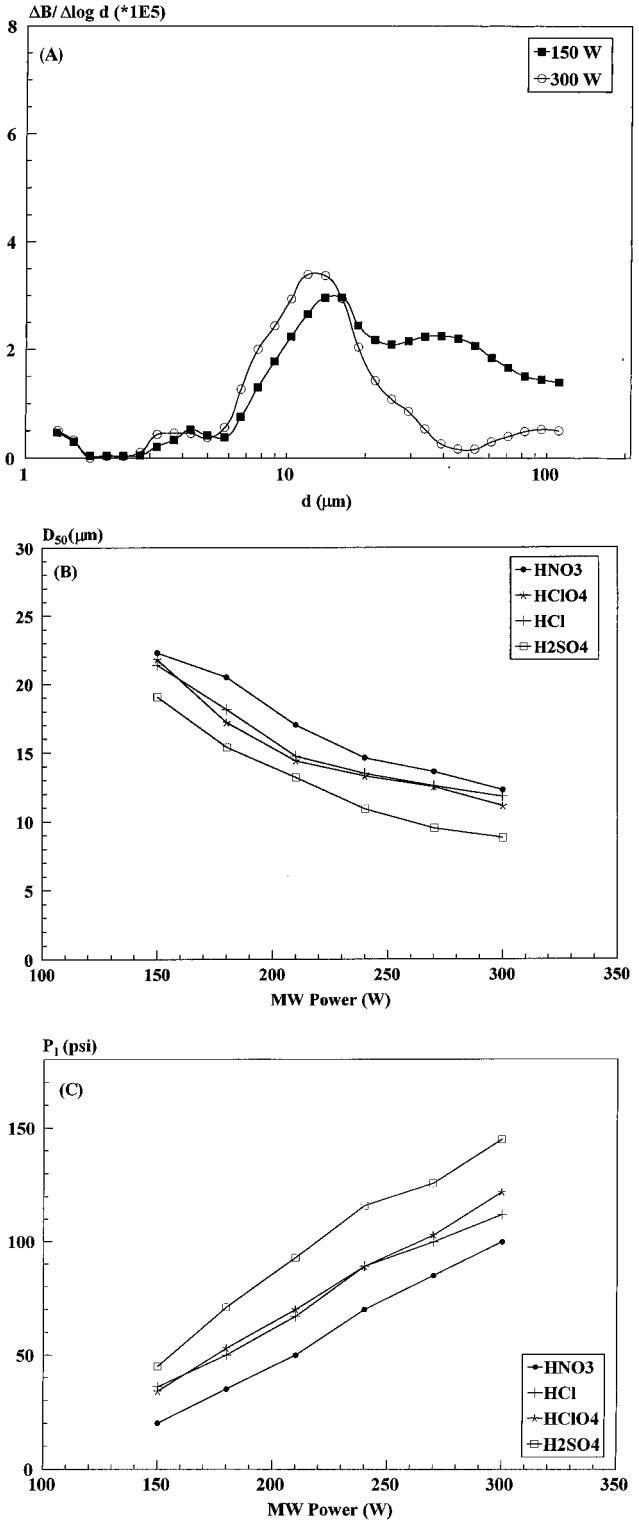

Figure 2. Effect of the MW power on (A) absolute pDSD curves of nitric acid solutions; (B) D_{50}; (C) P_1. $Q_1 = 2$ mL/min, $L = 30$ cm, outlet capillary of 100 μm i.d., and acid concentration of 0.75 M.

dispersion of the drop size diameters, it does not seem to change with power, since there always exists a given volume of aerosol distributed along the whole measurement interval of the instrument. Figure 2A is very helpful in order to quantitatively predict what set of experimental conditions will give rise to greater losses in the introduction system. To this end, the nebulization chamber could be considered as a filter that prevents drops of over 20 μm to pass, under the usual ICPAES conditions (this would be the so-called "cutoff" diameter of the introduction system, d_c).[2,23] If one assumes that this is the actual value in our introduction system (obviously, it will be somewhat lower, due to the presence of the condenser unit), Figure 2A allows one to predict that the maximum loss of aerosol will probably be at 150 W.

In those cases in which the width of the curve does not make it possible to establish which pDSD shows a lower size dispersion, it is useful to employ a parameter such as the span.[21,22] For the distributions shown in Figure 2A, the span values were 2.59 and 1.86, respectively, for 150 and 300 W. This points out that the pDSDs obtained with the MWTN are less disperse, in relative terms, at high than at low power values, although the percentage of liquid volume contained in large drops is lower at high power values.

For all the acids tested, D_{50} values decrease as MW power is increased (Figure 2B). This behavior can be easily explained if one considers that, at a given liquid flow (Q_1), more power means a higher fraction of evaporated solvent and, hence, a lower fraction of remaining liquid sample to be nebulized. As is well-known in pneumatic nebulization, the aerosol becomes finer as gas flow is increased and liquid flow is decreased.[24−26] Besides, back pressure is expected to increase, since more volume of gas is forced to pass through the same bore (Figure 2C). In addition, there is a decrease in the area under the curves shown in Figure 2A, which means a decrease in the amount of liquid. This behavior is similar to that shown by the conventional thermospray when the control temperature of the capillary rises.[4,5,20]

As regards V_{20}, the values obtained become higher as MW power is increased (~50% at 150 W and ~85% at 300 W). This effect, and the fact that aerosols are less disperse, should tend to improve the transport rate.

It can be seen in Figure B and C that the above described behaviors are similar for all the acids tested.

(2) Influence of Liquid Flow. Figure 3A shows the pDSD curves of HNO_3 for three Q_1 values on an absolute volume basis, and Figure 3B the variations of D_{50} vs Q_1 for solutions 0.75 M in HNO_3, HCl, $HClO_4$, H_2SO_4, and H_3PO_4.

Figure 3A shows that the pDSD curves shift to smaller drop diameters as Q_1 is increased. These pDSD curves peak at 13.8 and 10.2 μm when Q_1 increases from 1.5 to 3 mL/min. At 3 mL/min, almost all the aerosol liquid volume is contained in droplets smaller than 34 μm in diameter, whereas at 1.5 mL/min there is a small aerosol liquid volume contained in droplets larger than 118 μm. For all the acids studied, the width of the pDSD decreases when Q_1 rises. As regards the pDSD dispersion, it has been observed that the span decreases when Q_1 is increased from 1.5 to 2.5 mL/min. For 3 mL/min, the variations are not so clear. Thus, for sulfuric acid, span values of 1.73 and 2.26 are obtained at 2.5 and 3 mL/min, respectively. This unexpected behavior is due to the fact that, when Q_1 is increased, the difference ($D_{90} - D_{10}$) decreases less markedly than D_{50} (i.e., from 2.5 to 3 mL/min, ($D_{90} - D_{10}$) varies from 10 to 9.77 μm, whereas D_{50} varies from 6.45 to 4.31 μm).

For all the acids, D_{50} decreases as Q_1 is increased. This behavior is similar to that shown by the conventional thermo-

(24) Canals, A.; Wagner, J.; Browner; R. F.; Hernandis, V. *Spectrochim. Acta* **1988**, *43B*, 1321−1335.
(25) (25) Browner, R. F.; Canals, A.; Hernandis, V. *Spectrochim. Acta* **1992**, *47B*, 659−673.
(26) Todolí, J. L.; Canals, A.; Hernandis, V. *Spectrochim. Acta* **1993**, *48B*, 373−376.

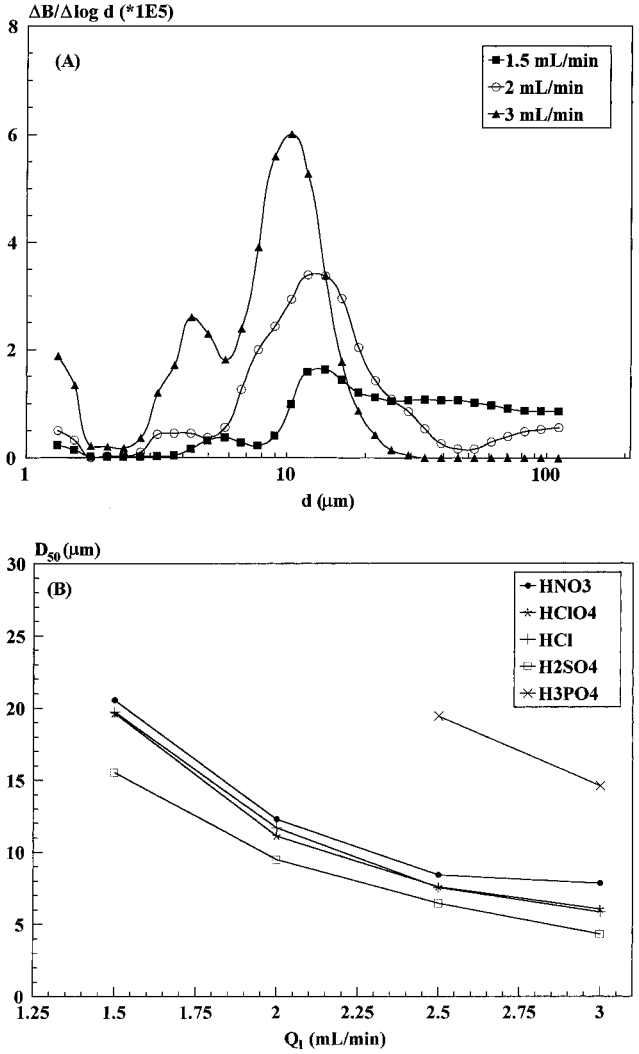

Figure 3. Effect of Q_1 on (A) absolute pDSD curves of nitric acid solutions and (B) D_{50}. L = 30 cm, outlet capillary of 100 μm i.d., MW power of 300 W and acid concentration of 0.75 M.

spray[4,5,20] and opposite to that of the concentric pneumatic nebulizers.[25−27] In the conventional thermospray, this behavior can be explained by taking into account that the fraction of solvent that is vaporized (F_v) is independent of Q_1[3,20] and hence the amount of liquid vaporized (i.e., the product $F_v \times Q_1$) increases with Q_1, so that the aerosol becomes finer.

With the MWTN, F_v values are expected to show little dependence on Q_1, since most of the MW absorption takes place before evaporation starts. Once evaporation has started, the velocity of the gas/liquid mixture is greatly increased, thus rapidly going beyond the irradiated length, so that little more MW absorption is expected to occur. Therefore, at low liquid flows, the liquid vein would travel a short distance within the irradiated length before evaporation starts, whereas at high liquid flows this distance would be longer. However, the irradiation times would not be very different from each other, and therefore F_v values would also be similar. Thus, when Q_1 is increased, the flow rate of nebulizing gas increases too. The pressure also increases, as expected, since more gas is forced to pass through the same bore. The pressure raised from ~50 psi at Q_1 = 1.5 mL/min to ~200 psi at Q_1 = 3 mL/min, for HNO_3, H_2SO_4, $HClO_4$, and HCl, and much less for H_3PO_4. Both facts, more gas and more pressure, contribute to obtaining finer aerosols (Figure 3).

For all the acids tested, V_{20} increases with Q_1, from ~50% at Q_1 = 1.5 mL/min to almost 100% at Q_1 = 3 mL/min, this increase being much lower (from 52 to 72%) for H_3PO_4. This is to say, for nitric, perchloric, hydrochloric, and sulfuric acids, when Q_1 > 2.5 mL/min, all the liquid aerosol volume is contained in droplets smaller than 20 μm.

(3) Influence of the Irradiated Length. It can be anticipated that increasing the irradiated length of the capillary (L) leads to an increased time of exposure to the radiation, although the relative increase in the time of exposure should be much lower than the relative increase of the irradiated length, owing to the fact that the velocity of the gas/liquid mixture steeply increases as evaporation takes place. A longer irradiation time should lead to higher F_v values (i.e., more gas and more pressure), which in turn should lead to finer aerosols.

Table 4 shows, at different liquid flows, the values of D_{50}, span, P_1, and V_{20} for two L and two MWTN with different inner diameters. It can be observed that when L is increased, lower D_{50} values are obtained. This is accounted for by the higher pressures obtained with L = 30 cm. As regards the drop size dispersion, and when using the 75 μm i.d., the higher the L values, the higher the span values. Again, this is due to more important changes in D_{50} (i.e., 19% for Q_1 = 2.5 mL/min and 17% for Q_1 = 3 mL/min) than in ($D_{90} - D_{10}$) (2 and 5%, respectively), when the irradiated length (L) is increased between 20 and 30 cm.

On the other hand, V_{20} values show no significant differences between L = 20 cm and L = 30 cm, always above 98% (Table 4).

(4) Influence of the Inner Diameter of the Outlet Capillary. The pDSD for two inner diameters on an absolute basis are also shown in Figure 4. When the inner diameter of the outlet capillary decreases, the pDSD shift to lower diameters. With the outlet capillary of 75 μm, all the aerosol volume is contained in droplets smaller than 19 μm whereas with a capillary of 100 μm this limit is 34 μm. This is the reason why the width of the pDSD is smaller with an i.d. of 75 μm (i.e., less dispersion in droplet sizes). Nevertheless, the span value is higher for a 75 μm i.d. (Table 4). This can be due to the above mentioned reasons.

On comparing the results obtained using two different outlet capillaries (Table 4), the lowest D_{50} values are always found for the narrowest capillary. This result is also consistent with previously published data obtained with conventional thermospray nebulizers[7,20] and can be explained by taking into account that, under the same set of experimental conditions, F_v, and hence the nebulizing gas flow, are about the same for both diameters, since

Table 4. D_{50}, Span, P_1, and V_{20} Values for the MWTN under Different Conditions[a]

L (cm)	i.d. (μm)	Q_1 (mL/min)	D_{50} (μm)	span	P_1 (psi)	V_{20} (%)
20	100	2.5	8.76	1.55	72	98
20	100	3.0	8.22	1.50	82	99
20	75	2.5	5.65	1.78	164	100
20	75	3.0	4.12	2.10	228	100
30	100	2.5	8.40	1.43	129	99
30	100	3.0	7.81	1.40	145	99
30	75	2.5	4.55	2.17	200	100
30	75	3.0	3.43	2.37	232	100

[a] Acid solution, 0.75 M HNO_3; MW power, 300 W.

(27) Nixon, D. E. *Spectrochim. Acta* **1993**, *48B*, 447−459.

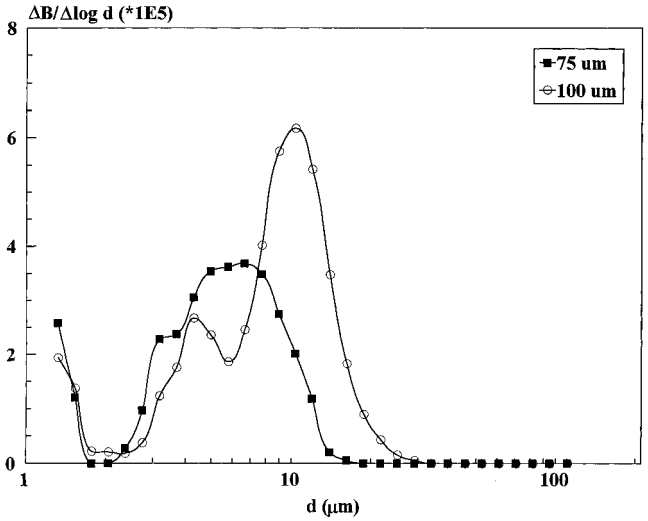

Figure 4. Absolute pDSD curves obtained with capillaries of different inner diameter. $Q_1 = 3$ mL/min, $L = 30$ cm, MW power of 300 W and nitric acid concentration of 0.75 M.

they depend mainly on the irradiation time, which is the same in both cases. As the pressure required to reach a given gas flow rate is much higher for the narrowest outlet capillary, the energy available for surface generation in this case will also be higher and, hence, the mean drop size smaller.[20,23,26−28]

It appears in Figure 4 that the area under the pDSD curve for an MWTN of 100 μm i.d. is higher than that of an MWTN of 75 μm. This unexpected behavior can be due to the fact that the aerosol velocity near the tip of the nebulizer increases on decreasing the inner diameter. Thus, the volume concentration is lowered and, therefore, also the value of the area under the pDSD curves. Moreover, the percentage of liquid volume of aerosol contained in droplets smaller than 1.2 μm, $V_{1.2}$ (which is higher for a 75 μm i.d.), is not included in the representations of Figure 4. Hence, since the $V_{1.2}$ values are 14 and 37% for the 100 and 75 μm i.d., respectively, the areas under the pDSD curves in Figure 4 are representative of 86 and 63% of the total aerosol liquid volume.

Finally, it is important to note that the V_{20} are slightly lower for the MWTN of 100 μm, although, in all the cases, these values are higher than 98% (Table 4).

(5) Influence of the Nature and Concentration of the Acid. Figure 5A shows the variation of D_{50} against the concentration of the acid for the five acids studied. With the exception of H_2SO_4, D_{50} values decrease as the acid concentration is increased for the entire acid concentration range evaluated. This behavior is due to the ease with which ionic solutions absorb MW radiation. The heating process is accelerated as the acid concentration is increased, thus giving rise to higher F_v and pressure values (Figure 5B), which, in turn, give rise to finer aerosols. The behavior of the H_2SO_4 is quite similar to that of the other acids, but a minimum in D_{50} values is obtained at a concentration of 3 M. At the same sulfuric acid concentration, a maximum for the P_1 values is observed.

As regards the nature of the acid, for acid concentrations lower than 3 M, the D_{50} values are as follows:

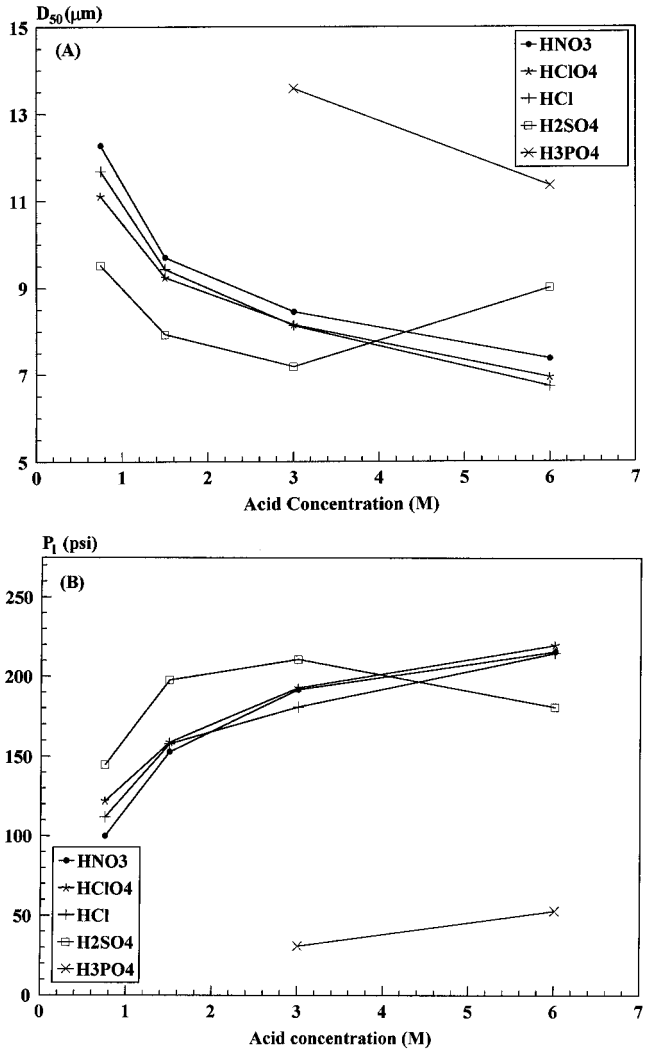

Figure 5. Effect of acid concentration on (A) D_{50} and (B) P_1. $Q_1 = 2$ mL/min, $L = 30$ cm, outlet capillary of 100 μm i.d., and MW power of 300 W.

$$H_2SO_4 < HClO_4 \cong HCl < HNO_3 \ll H_3PO_4 \qquad (1)$$

Some experiments were carried out to try to explain this behavior. In these experiments, acidic solutions (0.75 M) were forced to pass through an irradiated capillary length of only 15 mm, and their temperatures were measured at the exit of the MW oven. These experiments were repeated at different sample uptake rates (2−3 mL/min). In order to avoid vaporization, an outlet capillary of 500 μm and an applied power of only 30 W were initially used. The results proved that, at all the Q_1 evaluated, the final temperature of the solutions followed the order

$$H_2SO_4 > HClO_4 \cong HCl > HNO_3 \gg H_3PO_4 \qquad (2)$$

This means that some acids absorb MW radiation more easily than others. Hence, these acids are expected to provide higher F_v values and give rise to finer aerosols than the others, under the same conditions.

Some properties of the acid solutions are to be taken into consideration when trying to explain this behavior. One of these properties is the ionic strength (Table 1), since ion migration is one of the mechanisms of MW absorption.[16] However, the contribution of a given ion to MW absorption depends on its ionic

(28) Canals, A.; Hernandis, V.; Browner, R. F. *J. Anal. At. Spectrom.* **1990**, *5*, 61−66.

mobility. Among the ions present in the solutions employed, H_3O^+ is, by far, the one that shows the highest ionic mobility. Sulfuric acid solutions show the highest concentration of H_3O^+, at equal concentrations of the acid, so that they are expected to absorb MW radiation more efficiently than the rest of the acids. At the opposite end, phosphoric acid solutions show the lowest, by far, values of the H_3O^+ concentration, for the same acid concentration. Therefore, the contribution of the ionic migration to MW absorption, in this case, is expected to be quite low. In fact, when H_3PO_4 was used, nebulization was not possible under several of the experimental condition sets employed in this work (i.e., Q_1 < 2.5 mL/min and an acid concentration of <1.5 M). The H_3O^+ concentrations for hydrochloric, perchloric, and nitric acid solutions are identical, for the same acid concentration. In agreement with this, the D_{50} values of primary aerosols are quite similar (Figure 5A). The little differences among them can be assigned to the slightly different contribution of the anions, as well as to other physical properties of the solutions such as density or viscosity (Table 1). As expected, there is a good correlation between the D_{50} values (Figure 5A) and back pressure (Figure 5B). Thus, the acids that provide smaller D_{50} values are those that give rise to the highest back pressures and vice versa.

A specific comment is to be made about the behavior of highly concentrated solutions (i.e., 6 M) of sulfuric acid. This acid solution provides higher D_{50} and lower P_1 values than HNO_3, HCl, or $HClO_4$ at the same concentration. The reason for this is probably the high viscosity of the sulfuric acid solution in comparison to the rest of the acid solutions (Table 1), since viscosity hampers MW absorption through a reduction of the ionic mobility.[16] This way, heating and vaporization will proceed at a lower rate than expected. Under these conditions, the pressure achieved will be lower (Figure 5B) and the aerosols generated coarser than expected (Figure 5A). Moreover, in pneumatic nebulization, the influence of the viscosity is to increase the mean drop size of the primary aerosols,[22,25] so that this will also contribute, to some extent, to the results shown in Figure 5A for high H_2SO_4 concentration.

As regards V_{20}, an increase in the acid concentration gives rise to increases in this parameter for all the acids tested except for sulfuric acid, for which a slight decrease appears at concentrations above 3 M. At low concentrations, H_2SO_4 affords higher V_{20} values than the remaining acids.

(6) Comparison with a Conventional Pneumatic Nebulizer. The pDSDs on an absolute basis of the aerosols generated with the MWTN of 75 μm i.d. using a solution of nitric acid (0.75 M) are shown in Figure 6. The same graph shows the pDSDs obtained with the Meinhard nebulizer at two different gas flow rates, 0.54 and 0.87 L/min. The primary aerosol generated with the MWTN is finer and less disperse than those generated with the Meinhard nebulizer. With the former, the entire volume of aerosol is contained in droplets smaller than 19 μm while the Meinhard has an important fraction of aerosol volume contained in droplets larger than this value (i.e., 73 and 45% for 0.54 and 0.87 L/min, respectively).

The effect of the molecular weight of the nebulization gas on the pDSD has been previously reported.[24] In the case of MWTN, the aerosol is generated by the action of solvent vapor (i.e., mainly water vapor), whereas for the Meinhard it is argon. According to this, the aerosols generated with the latter should be finer. Therefore, this behavior is most likely due to the higher operating

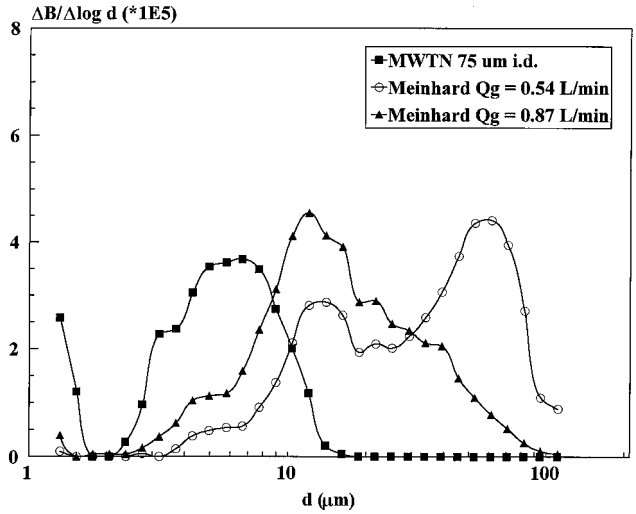

Figure 6. Absolute pDSD curves for MWTN (L = 30 cm, outlet capillary of 75 mm i.d., and MW power of 300 W) and Meinhard nebulizer at two different Q_g. Q_1 = 3 mL/min; nitric acid concentration 0.75 M.

pressure and to a more efficient interaction between gas and liquid streams associated with the MWTN. Taking a d_c of 20 μm,[23] Figure 6 reveals that, for the MWTN, all the aerosol would be transported to the atomization cell. For this reason, with this nebulizer it is advisable to use a desolvation unit in order to reduce the solvent load to the plasma. Obviously, a condensation system, similar to the one employed in the present study, will reduce the analyte transport rate to the plasma and the signal improvements will be less important than expected.[29]

Analytical Signal. The analytical sensitivity in ICPAES depends, to a great extent, on the characteristics of the primary aerosol that determine the analyte transport rate. Analyte transport rate is favored when the aerosol mean drop size is small and also when its dispersion is low, since coalescence increases with the aerosol dispersion.[30−32]

The results shown in the previous section have proved that, with the MWTN, the higher the acid concentration, the finer and less disperse the aerosols generated, with the exception of sulfuric acid at high concentration. However, such very high acid concentrations would deteriorate the excitation conditions of the plasma,[33] so that the sensitivity enhancement associated with the increase of the acid concentration would be much lower than expected from the concomitant improvement of the aerosol characteristics. Because of this, emission signal measurements have been done using the lowest of the acid concentrations studied (i.e., 0.75 M). It is worth mentioning that, even with these acid concentrations, the MWTN generates finer and less disperse aerosols than the Meinhard nebulizer (Figure 6). In addition, the acid load to the plasma is further reduced by the use of a condensation unit.

Figure 7 shows the net emission intensity of Mn II vs Q_1, for MWTN and Meinhard nebulizers. Nitric acid was the only one

(29) Tarr, M. A.; Zhu, G.; Browner, R. F. *J. Anal. At. Spectrom.* **1992**, *7*, 813−817.
(30) Canals A.; Hernandis, V.; Browner, R. F. *Spectrochim. Acta* **1990**, *45B*, 591−601.
(31) Liu, H.; Montaser, A. *Anal. Chem.* **1994**, *66*, 3233−3242.
(32) Hinds, W. C. *Aerosol Technology*; Wiley: New York, 1982.
(33) Canals, A.; Hernandis, V.; Todolí, J. L.; Browner, R. F. *Spectrochim. Acta* **1995**, *50B*, 305−321.

Table 5. Figures of Merit in ICPAES[a]

element	$I_{MWTN}/I_{Meinhard}$		LOD[b] (ng/g)			$BEC_{Meinhard}/BEC_{MWTN}$[b]	
	MWTN75	MWTN100	Meinhard	MWTN75	MWTN100	MWTN75	MWTN100
Al	1.8	1.3	73	41	54	0.9	0.9
Ba	2.1	1.9	2.0	1.0	1.4	1.6	1.7
Ca	1.7	1.5	6.7	3.9	3.9	1.5	1.3
Cd	1.5	1.1	30	15	26	1.4	1.0
Cr	2.3	2.1	85	37	40	1.3	1.4
Cu	1.6	1.6	5.2	3.3	3.6	1.1	1.0
Fe	2.1	2.0	12	5.6	5.9	1.5	1.4
Mg	2.5	2.1	2.7	1.1	1.3	1.1	1.0
Mn	2.8	2.1	7.4	2.5	3.4	2.0	1.9
Zn	1.7	1.0	4.8	20	33	1.4	1.2

[a] Solvent: HNO_3 0.75 M; Q_l = 3 mL/min; Q_g (carrier/nebulizer) = 0.54 L/min; MW power, 300 W; L = 30 cm. [b] Calculated as 3 times the standard deviation from 10 readings of the blank.

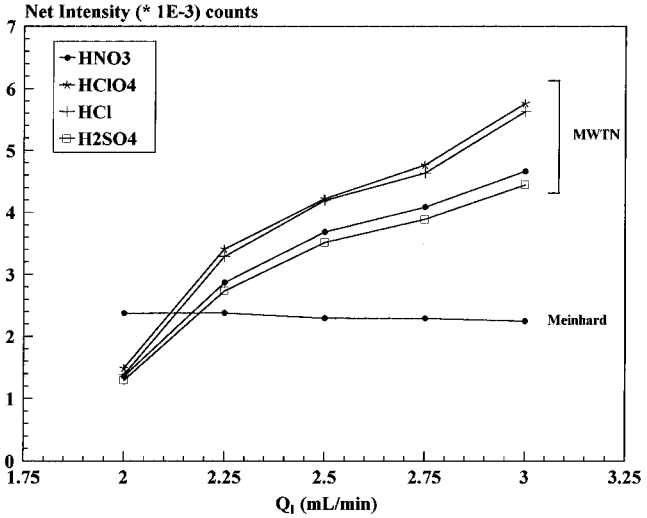

Figure 7. Variation of the net emission intensity of Mn II vs liquid flow rate. Acid concentration 0.75 M. MWTN: outlet capillary of 100 μm i.d., L = 30 cm, and MW power of 300 W. Meinhard nebulizer: Q_g = 0.54 L/min.

used with the Meinhard nebulizer, given that the signals obtained for all the acids at 0.75 M were similar with this type of nebulizer. For all the acids evaluated with the MWTN, emission intensity increases greatly with Q_l, whereas it remains constant for the Meinhard nebulizer. As Q_l is increased, the primary aerosol obtained with the MWTN becomes finer (Figure 3) and a higher percentage of its volume is contained in droplets smaller than 20 μm, so that the analyte transport efficiency (ϵ_n) is expected to increase. Since the analyte transport rate is

$$W_{tot} = Q_l \epsilon_n C_n \quad (3)$$

where C_n is the analyte concentration, W_{tot} increases with Q_l. For the Meinhard nebulizer, the primary aerosol becomes a little bit coarser as Q_l is increased, so that ϵ_n is expected to decrease, as has been experimentally proven. Therefore, W_{tot} is not expected to show a significant variation.[26]

As regards the acid employed, Figure 7 shows that the emission intensities obtained with perchloric and hydrochloric acids are always somewhat higher than those obtained with nitric acid. When Q_l is increased from 2.0 to 3.0 mL/min, net intensity increases by a factor of 3.4 for the combination MWTN-HNO_3 and by a factor of 3.9 for MWTN-$HClO_4$. Once again, this result is in good agreement with the results of aerosol characterization (Figure 3B). Figure 7 also shows that sulfuric acid (0.75 M) gives rise to the lowest net emission intensities in spite of having provided the finest aerosols (Figures 2B, 3B, and 5A). This effect could be explained by the excessive solvent transport caused by the fineness of the primary aerosol and the intensification of nucleation processes (i.e., there are more condensation nuclei and vapor).[32] On the other hand, sulfuric acid causes a more important interference effect on the thermal characteristics of the plasma.[33]

The net intensity observed when the MWTN was used was generally higher than when the Meinhard nebulizer was used. Only at 2.0 mL/min was the emission intensity obtained with the Meinhard nebulizer higher than that with the MWTN. These results can be explained by taking into account the different aerosol transport devices used for both nebulizers (i.e., the condensation device for MWTN and the Scott spray chamber for the Meinhard nebulizer) since primary aerosols generated by the MWTN are, in all cases, finer than those obtained with the Meinhard nebulizer.

Finally, Table 5 gathers, for both nebulizers, some important figures of merit (i.e., relative emission intensities ($I_{MWTN}/I_{Meinhard}$); absolute limits of detection ($LOD_{Meinhard}$, LOD_{MWTN}), and relative background equivalent concentrations ($BEC_{Meinhard}/BEC_{MWTN}$)) for 10 elements of different excitation and ionization energies. The relative emission intensities lie between 1.0 and 2.8, depending on the element and on the inner diameter of the outlet capillary of the MWTN. The intensity obtained with the capillary of 75 μm is always higher than with that of 100 μm, as expected from the characteristics of their primary aerosols (Figure 4). At a Q_l of 3 mL/min, the instrumental limits of detection are always better for the MWTN in comparison with the Meinhard nebulizer. This was likely the result of the higher analyte transport rate when the MWTN is used, which leads to a larger concentration of analyte in the observation zone together with similar or lower average background emission intensities. BEC values are smaller for the MWTN than for the Meinhard nebulizer, with the exception of Al. As expected, the narrower outlet capillary affords the lowest LODs. Finally, when the same sample introduction system is used with both nebulizers (i.e., condensation system), the sensitivities obtained with the MWTN are higher (2.3−6.2 times), the LODs lower (1.8−5.5 times) and the BECs also lower (1.2−4.4 times) than those obtained with the Meinhard nebulizer.

CONCLUSIONS

The results shown in this work confirm that MW radiation can be successfully used for the liquid sample introduction in ICPAES. The D_{50} and the dispersion of the primary aerosols generated using the MWTN decrease whereas V_{20} increases as the MW power is increased, as the liquid flow is increased, as the irradiated length of the capillary is increased, as the inner diameter of the outlet capillary is reduced, and as the strength and concentration of the acid are increased. In general, under the conditions studied, the primary aerosols are always finer than those obtained with a standard Meinhard nebulizer, working under the same set of conditions.

With the MWTN, an increase in Q_1 leads to increases in the ICPAES emission intensity. Sulfuric acid generates the finest primary aerosols but it gives lower emission intensities than the remaining acids. The MWTN affords higher sensitivity and lower limits of detection than the standard Meinhard nebulizer.

This type of nebulization features many of the advantages of the conventional thermospray nebulizer and overcomes some of its drawbacks (no corrosion problems, lower working pressure, aerosol characteristics not modified when the PTFE capillary is replaced, etc.). Some previous experiments have been performed on the nebulization of high salt content solutions (NaCl 20%, w/w). No clogging has been observed with the MWTN. These results will be presented in future articles.

Finally, it should be pointed out that this work has been carried out with a first prototype of the MWTN. Several modifications are currently being developed in our laboratories (e.g., using a peristaltic pump instead of an HPLC pump, to reduce cost, improving the aerosol transport system). These results will also be presented in a near future.

ACKNOWLEDGMENT

The authors express their appreciation to the DGICyT (Grants PB92-0336 and PB95-0693 Spain) for financial support. Presented at the 1996 Winter Conference on Plasma Spectrochemistry. Fort Lauderdale, FL, January 1996.

LIST OF SYMBOLS AND DEFINITIONS

BEC_i	background equivalent concentration obtained with the nebulizer *i*
D_{10}	diameter at 10% volume point
D_{50}	median of volume drop size distribution (i.e., diameter at 50% volume point)
D_{90}	diameter at 90% volume point
F_v	fraction of solvent vaporized
I_i	net emission intensity obtained with the nebulizer *i*
L	capillary irradiated length
LOD_i	limit of detection obtained with the nebulizer *i*
MWTN	microwave-powered thermospray
pDSD	drop size distribution of primary aerosol
P_1	back pressure of HPLC pump
Q_g	nebulizing/carrier gas flow rate
Q_1	sample uptake rate
span	measure of the width of the volume distribution relative to the median diameter (i.e., $(D_{90} - D_{10})/D_{50}$)
VC	volume concentration
$V_{1.2}$	percentage of liquid volume of aerosol contained in droplets smaller than 1.2 μm
V_{20}	percentage of liquid volume of aerosol contained in droplets smaller than 20 μm
ΔB	VC × (percent of the aerosol volume in band)
$\Delta B/\Delta \times \log d$	volume of aerosol corresponding to a given drop size

Received for review December 10, 1996. Accepted June 1, 1997.[⊗]

AC961247A

[⊗] Abstract published in *Advance ACS Abstracts,* August 1, 1997.